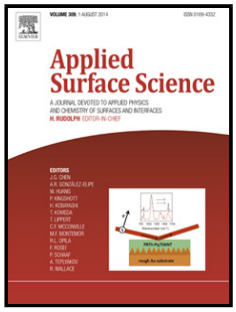

Title: $Ti_{1-x}Ag_x$ electrodes deposited on polymer based sensors

Author: S.M. Marques N.K. Manninen Stanislav Ferdov S. Lanceros-Mendez S. Carvalho

PII: S0169-4332(14)01920-5
DOI: http://dx.doi.org/doi:10.1016/j.apsusc.2014.08.142
Reference: APSUSC 28597

To appear in: *APSUSC*

Received date: 3-4-2014
Revised date: 9-6-2014
Accepted date: 25-8-2014

Please cite this article as: S.M. Marques, N.K. Manninen, S. Ferdov, S. Lanceros-Mendez, S. Carvalho, $Ti_{1-x}Ag_x$ electrodes deposited on polymer based sensors, *Applied Surface Science* (2014), http://dx.doi.org/10.1016/j.apsusc.2014.08.142

Graphical Abstract

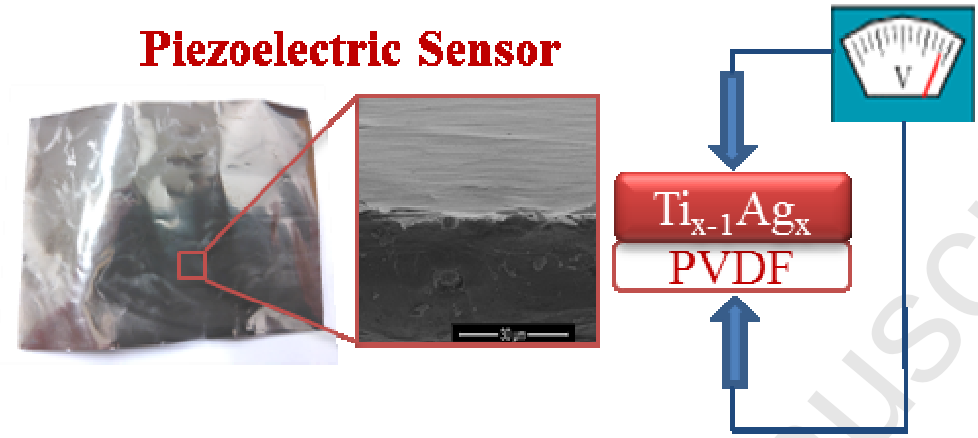

Highlights

- $Ti_{1-x}Ag_x$ thin films with diverse Ag/Ti ratios were deposited by sputtering on piezoelectric PVDF;
- The deposition conditions do not promote changes on the polymer structure;
- The coatings do not change the piezoelectric properties of the polymer;
- Sheet resistivity values show a typical behavior of a binary alloy system.
- The deposited films as suitable for the development of functional electrodes

$Ti_{1-x}Ag_x$ electrodes deposited on polymer based sensors

S. M. Marques [a]*, N. K. Manninen [b], Stanislav Ferdov [a], S. Lanceros-Mendez [c], S. Carvalho [a, b]

a - GRF-CFUM, Physics Department, University of Minho, 4800-058 Guimarães, Portugal

b - SEG-CEMUC Mechanical Engineering Department, University of Coimbra, 3030-788 Coimbra, Portugal

c - Physics Department, University of Minho, 4700-057 Braga, Portugal

*__Corresponding author:__

Sandra Mariana da Silva Marques

Universidade do Minho, Dept. Física, Campus de Azurém, 4800-058 Guimarães, Portugal

Tel: +351- 253510175 ext. 517469

Fax: +351-253510461

Email: mariana.marques@fisica.uminho.pt

Abstract

Piezoelectric materials are interesting for the development of sensors and actuators for biomedical applications in areas such as smart prosthesis, implantable biosensors and biomechanical signal monitoring, among others. For acquiring or applying the electrical signal from/to the piezoelectric material, suitable electrodes can be produced from Ti based coatings with tailored multifunctional properties: conductivity and antibacterial characteristics through Ag inclusions. This work reports on $Ti_{1-x}Ag_x$ electrodes with different Ag/Ti atomic ratios deposited by d. c. and pulsed magnetron sputtering at room temperature on poly(vinylidene fluoride), PVDF. The X-Ray Diffraction (XRD) results revealed that the deposition conditions preserve the polymer structure and suggested the presence of crystalline Tiβ phase in pure titanium coating and fcc-Ag phase in pure silver coating. According to the results obtained from scanning electron microscopy (SEM) analysis, the coatings are homogeneous and no clusters were found; since β-PVDF is anisotropic, the deposited coatings replicate the underlying substrate surface. Sheet resistivity values show a typical behavior of a binary alloy system, with low resistivity values for coatings of zone 1 (Ti rich) and zone 3 (Ag rich) and a slightly higher resistivity values in zone 2. The piezoelectricity of the different samples show similar values.

Keywords: Sensors, Ag nanoparticles, piezoelectric polymers, sputtering.

1. Introduction

Implant failure represents a large problem for both patients and health agencies, since it results in repeated surgeries with consequent discomfort and human pain, being also responsible for a large economic burden for society. This failure can be attributed to excessive wear and wear debris and also to microbial infection [1]. The future of prosthetic implants pass through the implementation of prevention mechanisms based on the implementation of sensor systems, which allow to obtain valuable information about a wide range of biomechanical signals [2,3]. An example of this evolution relays on piezoresistive [4,5] and piezoelectric materials to serve as strain and force sensor [6] for various applications. These sensors are suitable for the above-mentioned application, adding the fact that the piezoelectric materials do not need external power supply, being even able to provide energy to the circuit, keeping the system operational for longer periods of time [7,8].

Poly (vinylidene fluoride), PVDF, is well-known for its piezo and pyroelectric properties, useful for a wide variety of applications in the field of sensors and actuators. For the four known polymorphs of PVDF, the β phase is the one with the largest piezoelectric response [9,10] and it was the one used as substrate material in this work. This phase can be obtained in different ways [9], being the most common the uniaxial stretching of α-phase (non electroactive) PVDF [11,12]. Further, for improving the piezoelectric response, the material must be poled, i.e. the alignment of the randomly organized dipolar moments against the applied electric field [11,12].

As this piezoelectric material transforms mechanical loads into electrical signals, conductive electrodes are necessary on both sides for signal acquisition. Such electrodes must show good electrical conductivity and since they are to be used within the human body they must be biocompatible. Titanium and its alloys have been widely used on artificial implants due to their

biocompatibility and good corrosion resistance [13], and Ti shows electrical conductivity in the range 43 μΩ cm [14].

Still, these implants show a high failure rate, mainly caused by microbial adhesion and colonization [13]. Thus, it becomes essential to create strategies that prevent bacterial adhesion in the first place. In addition, infections caused by *Staphylococcus* and other coagulase-negative *Staphylococci* (CNS) are also known as one of the most common causes of serious hospital acquired infections [13,15]. This is related to the ability of microorganisms to adhere to medical devices and forming biofilm. Despite various efforts to develop effective medical treatments against infections caused by biofilms [16], the physical removal of an infected medical device (such as implants) is often necessary, which entails extra costs, as well as physical discomfort of the patient. Over the past years a considerable interest in increasing biodevices lifetime, trough inhibition of biofilm, has raised. In order to achieve this goal, different concepts based on the incorporation of Ag in nanoparticles and coatings have been proposed, due to the effective antibacterial activity of this metal [13,17–19].

Presently, different coatings produced by magnetron sputtering are proposed as potential candidates as functional conductive electrodes in polymeric sensors. Regarding biomedical applications, TiNAg [20–22] and TiAg [14,23] coatings have been proposed for prosthesis pressure sensors and dry biopotential electrodes, respectively, due to their interesting electrical and biological properties. However, in the above mentioned reports the coatings were deposited on silicon and glass substrates. In fact, the high temperatures associated with sputtering process represent the major limitation in the development of functional electrode coatings in piezoelectric PVDF substrates, due to the eventual structural changes promoted by temperature as well as eventual depolarization of the sample, leading to the loss of the piezoelectric response.

Thus, the major innovation of the present report is the deposition of $Ti_{x-1}Ag_x$ electrodes on PVDF substrates, while maintaining the piezoelectric response of the polymer.

This report focus on the development of polymer based sensors for biomedical devices, which allow detecting early failure and/or to monitor implants and biomechanical signals. Taking into account the good electrical conductivity of Ti and Ag, $Ti_{1-x}Ag_x$ coatings represent a good candidate for electrode materials. In addition, Ti is biocompatible, while Ag has been pointed as an effective antibacterial agent, able to improve the lifetime of the biodevices. Thus, Ti, Ag and $Ti_{1-x}Ag_x$ coatings, with different Ag/Ti atomic ratios were deposited by magnetron sputtering in piezoelectric PVDF substrates. The electric and piezoelectric responses of these thin films were evaluated, together with their structure and morphology.

2. Materials and methods

$Ti_{1-x}Ag_x$ coatings were deposited by dc/pulsed dc magnetron sputtering onto ultrasonically cleaned silicon (used for AFM, and EPMA tests) and PVDF thin films with a thickness of approximately 28 μm (used for SEM, XRD analysis, Four Point Probe technique and piezoelectric response (d_{33}) tests) . One pure Ti target (99.99 %) and one Ag target (99.99%)) (both with 200x100 mm^2) were used in argon atmosphere with the substrates rotating at 70 mm from the target at a constant speed of 7 rpm. During deposition, the pressure in the deposition chamber was about 0.17 Pa and the argon flow was kept constant at 60 sccm. To vary the Ag content in the films, the current density applied to each target was varied, as indicated in Table 1. The Ti target was connected to the pulsed dc power supply, while the Ag target was connected to a dc power supply. For the deposition of the pure silver coating and the $Ti_{1-x}Ag_x$ coating with lowest Ag content (coating Ag/Ti 0.02) the pulsed dc power supply was connected to the Ag

target and for the latter case the dc power supply to the Ti target. The frequency and reverse time were fixed at 200 kHz and 1536 ns, respectively, corresponding to a duty cycle of 69 %. The deposition time was varied in order to obtain a final thickness ranging between 150 nm to 200 nm. In order to avoid the structural damage of the polymer substrate, the substrate temperature must be ideally kept below ~100ºC- (far from the melt transition temperature of PVDF) [9]. In this sense, the depositions were performed without any external heating of the substrate and no bias polarization was applied on the substrate holder.

Chemical characterization was performed with a Cameca SX 50 electron probe microanalysis (EPMA) apparatus. Five punctual measurements were randomly performed on the samples surface, with an acceleration voltage of 10 kV. Since the depth of analysis at 10kV is about 300 nm for pure Ag and 700 nm for pure titanium, $Ti_{1-x}Ag_x$ coatings with a thickness of 1 μm were deposited for EPMA analysis. The morphology/topography of the coatings, was evaluated by atomic force microscopy (AFM) using a NanoScope III apparatus (Digital Instruments) operating in tapping mode. AFM images were taken over scanning areas of 5 × 5 μm^2. The roughness values are an average of three measurements. The surface morphology and thickness were by examined by scanning electron microscopy (SEM) with a NanoSEM – FEI Nova 200 (FEG/SEM). The structure and phase distribution of the coatings were analyzed by powder X-rays diffraction (XRD) using a Bruker D8 Discover diffractometer (CuKα radiation – λ =1.5406 Å, step 0.04º, time per step 1s and 6-60 2θ interval). The sheet resistivity was tested by Four Point Probe technique, in three randomly distributed points with a d. c. current and voltage calibrator. The piezoelectric response (d_{33}) of the poled samples was analyzed with a wide range d_{33}-meter (model 8000, APC Int Ltd).

3. Results and discussion

3.1 Chemical composition vs. deposition parameters

The synthesis conditions together with the coating´s chemical composition, deposition rate, roughness and sheet resistivity are summarized in Table 1.

Through the deposition time and coatings thickness, estimated by SEM analysis, it was possible to determine the deposition rate. The $Ti_{1-x}Ag_x$ coatings were labeled according to the Ag/Ti atomic ratio, while pure titanium and pure silver coatings are labeled as Ti and Ag, respectively. The coatings were divided in three different zones: Z1 (Ag/Ti < 0.11), Z2 (0.11<Ag/Ti>0.69) and Z3 (Ag/Ti>0.69) according to the variations in the resistivity values.

Since Ag and Ti show high sputtering yields (3.12 and 0.51, when bombarded with Ar at 0.5 keV, respectively [24]) the deposition of these elements results in high deposition rates. The use of pulsed dc power supply promotes a reduction in the deposition rate, thus, allowing to control the chemical composition of the coatings, achieving a low Ag content, in the case of Ag/Ti (0.02), and low Ti contents in the coatings of zone 3. As shown in Table 1, the J_{Ag} applied on the Ag target was 0.05 mA/cm^2 for the deposition of Ag/Ti (0.02) and Ag/Ti (0.11), however, in the first case the pulsed dc power supply was connected to the Ag target, while in the coating with Ag/Ti (0.11) the dc power supply was connected to the Ag target. Despite the similar current density applied to Ag target (J_{Ag}) and the decrease on the current density applied to Ti target (J_{Ti}) in the deposition of Ag/Ti(0.11), the silver content was five times higher in relation to the coating Ag/Ti (0.02), which demonstrates the reduction in the sputtering rate with the use of pulsed dc power supply, as used on Ag/Ti (0.02) sample deposition.

Regarding the coatings deposited in similar deposition conditions (with a pulsed dc and a dc power supply connected to Ti and Ag targets, respectively) it can be found from Figure 1 that the Ag content increases linearly with the J_{Ag}/J_{Ti} ratio, along with a decrease in the Ti content.

The relation between current density and sputter efficiency is well described in [25] discussing that higher current densities applied on Ti and other material targets induce the sustained self-sputtering (SSS) effect meaning that during target bombardment by inert gas, in this case Argon (Ar), secondary electrons, photons, neutral and excited particles are extracted from target surface contributing to sputtering along with the inert gas, promoting a higher sputter effect [25]. According to the chemical composition, it is observed that with increasing current density applied on Ag target, the Ag content increases being this effect already explained on the previous topic.

3.2 Structural analysis

The crystalline structure of the coatings was evaluated by means of XRD analysis and the results are shown in Figure 2, where the main identified crystalline phases are depicted, namely Tiβ (ICDD181718) and Ag (ICDD 181730), together with the crystalline peaks of PVDF [9]. The XRD analysis was performed on pure Ti and Ag coatings and also in $Ti_{1-x}Ag_x$ coatings representative of the different zones defined previously.

XRD peaks corresponding to atomic planes (200) and (110) of β-PVDF (Figure 2a) indicate that the deposition conditions do not induce any phase change in the polymer. This means that the piezoelectric phase of PVDF is still present, and that, if not depoling of the material is induced during the deposition of the films, the piezoelectric response will be maintained (see later, Section 3.4). It can be seen a peak shift to the left, possible due to the compressive residual

stress in the coatings [26]. Pure Ti coating crystallizes in a hexagonal closed packed structure, which represents the most stable titanium phase [27–29]. The XRD pattern of Ag coating suggests the presence of crystalline fcc-Ag. A magnification of the XRD patterns are shown in Figure 2b, where the Ag, Ti, TiAg (ICDD 605934) and Ti_2Ag (ICDD 605935) crystalline peaks are identified. According to Figure 2a) and b) the $Ti_{1-x}Ag_x$ coatings present very similar XRD patterns, with the most intense peak at about 37.8º, which is close to the TiAg (013) diffraction peak. The formation of TiAg phase was previously reported for TiAg coatings deposited by magnetron sputtering [14]. However, taking into account that the titanium, silver and TiAg peaks show similar values, it is difficult to accurately identify the presence of the different phases. In the Ag/Ti(0.11) coating, in addition to the TiAg phase, the presence of Ti(002) peak can also be identified, which suggests that the coating is composed by a mixture of crystalline TiAg and Ti phases. This was somehow predictable since the amount of Ti present in the coating is high (89.8 at.%), which means that the TiAg phase is formed until the Ag is consumed and the remaining titanium forms a crystalline Ti phase. Regarding the coatings with higher Ag contents (40.8 at.% Ag (Ag/Ti(0.69)) and 78.8 at.% Ag (Ag/Ti(3.71)), it can be found that the diffraction peak of Ti(002) disappears, which suggests that the crystalline titanium phase is not present in these coatings. In fact, the diffraction patterns of $Ti_{1-x}Ag_x$ coatings representative of zone 2 and 3 are very similar, both showing comparable full width at half maximum (FWHM). The only difference in these two coatings is the presence of a diffraction peak at about 43º for the coating Ag/Ti(3.71) (see Figure 2a), which corresponds to the diffraction peak of TiAg(110), thus suggesting a change in the orientation. The diffraction patterns of Ag/Ti(0.69) and Ag/Ti(3.71), suggest the presence of TiAg phase, however, the presence of both Ti and Ag cannot be

discarded, especially for the coating with higher Ag content, where Ag phases should be present taking into account the high Ag content (78.8 at.%).

3.3 Topography and Morphology

SEM and AFM analyses were performed in order to evaluate surface characteristics and the presence of Ag nanoclusters on the surface. The SEM micrographs of coatings representative of different Zones (identified in Figure 1) are depicted in Figure 3.

Since β-PVDF is anisotropic, the deposited thin film ($Ti_{1-x}Ag_x$) replicates the underlying substrate surface showing a preferential accumulation of thin film along the crest of the longitudinal polymer microstructure obtained during the mechanical stretching to obtain the β polymer phase [9,12,30]. The co-deposition of Ag and titanium nitride (TiN) [31]; carbonitride (TiCN) [32] and oxide (TiO_2) [33] results in the formation of nanocomposites whit Ag nanoparticles embedded in the matrix coating, being the size of these nanoparticles strongly dependent on the amount of silver incorporated in the coating. The formation of Ag nanoparticles is related to the immiscibility of Ag in these matrixes. It was reported [14] that TiAg coatings were composed of TiAg clusters segregated from the Ti hexagonal grain boundaries, which appear as bright spots in SEM micrographs. In order to clarify if clusters of different phases (Ag or TiAg) were present, SEM analysis was performed with magnifications up to 200.000x (not shown) and also in backscattered electron mode (BSE) (shown in the inset), which allows to obtain the elemental contrast between elements of different atomic mass, where heavier phases should appear brighter. The XRD analysis suggested the formation of crystalline TiAg phases, combined with crystalline Ti phase (coatings of zone 1) and the formation of TiAg phases possibly combined with Ag and Ti phases in the coatings of zone 2 and 3. According to

the results obtained from SEM analysis (Figure 3), the coatings are homogeneous and no clusters were found.

Figure 4 shows AFM images of the Ti; Ag and $Ti_{1-x}Ag_x$ films deposited on silicon. The AFM images suggest that the coatings of zone 1 and zone 3 show similar morphologies, with roughness values between 3 nm to 5 nm, while the coating of zone 2 shows a smoother surface with a slightly lower roughness value (2 nm). Still, no large variations are observed between the tested coatings.

3.4 Sheet resistivity and piezoelectric d_{33} response

Figure 5 shows the coatings resistivity and piezoelectric response as a function of silver content in the coatings. Sheet resistivity shows a typical behavior of a binary alloy, according to literature [34].

When Ag is added to titanium, the sheet resistivity will increase with increasing Ag concentration. It is apparent that when it reach 100 at. % of Ag and consequently 0 at. % of Ti, the electrode behaves as a pure metal so the resistivity must be small. So the resistivity vary from 10.62 Ω/sq for 100 % of Ti and 0.12 Ω/sq for 100% of Ag. Therefore, resistivity versus Ag content must pass through a maximum, which for the Ti-Ag alloy is around ≈ 40 at. %. The coated polymer piezoelectric d_{33} response as a function of silver content is similar for the different samples. The values of the piezoelectric response vary from 19.6 pC N^{-1} to 27.6 pC N^{-1}. Taking into account the typical range of piezoelectric d_{33} values obtained for this materials [9], it is concluded that the deposition process does not modify the piezoelectric response of the material [30]. Thus, the electrodes deposited by sputtering on the PVDF surface under the

conditions proposed in this investigation, allow maintaining the functional piezoelectric response of the polymer and its use for sensor and actuator applications.

4. Conclusions

Ti, Ag and $Ti_{1-x}Ag_x$ thin films with different Ag/Ti atomic ratios were deposited on piezoelectric PVDF polymers by magnetron sputtering. The main goal of this investigation is to determine: i) if it is possible to deposit electrodes in PVDF polymeric films without causing any structural damage on the polymeric substrate and keeping the piezoelectric properties inherent to PVDF and ii) to evaluate the effect of thin films composition on the electrical response of PVDF coated sensors.

$Ti_{1-x}Ag_x$ thin films were divided in three different zones, according to the variations in the chemical composition, structure and electrical response: zone 1, with Ti rich coatings, with Ag/Ti atomic ratios ranging from 0 to 0.11, zone 2 which consists in a mixture of Ag and Ti (with Ag/Ti between 0.22 and 0.69) and zone 3, with silver rich coatings (Ag/Ti atomic ratios ranging from 1.27 to 3.71). XRD analysis suggested the presence of crystalline Tiβ phase in pure titanium coating and fcc-Ag phase in pure silver coating. The coatings of zone 1 are characterized by the presence of crystalline TiAg phase and Tiβ phase, while $Ti_{1-x}Ag_x$ thin films of zone 2 and zone 3 show similar XRD patterns, which suggest the formation of TiAg phase. However, since all the possible crystalline phases (Ti,Ag and TiAg), show very similar XRD patterns it is difficult to accurately identify the phases present in these thin films. Another important feature is the presence of β-PVDF phase diffraction peaks, which indicate that the deposition conditions did not damage the polymeric substrate. SEM images revealed that the topography of the anisotropic polymer (β-PVDF) tends to enhance a preferred nucleation of the

$Ti_{1-x}Ag_x$ thin films on the longitudinal crest of the polymer microstructure. The AFM analysis suggested that the coatings show very similar morphologies, with surface roughness ranging from 2 nm to 5 nm.

Sheet resistivity values show a typical behavior of a binary alloy system, with low resistivity values for coatings of zone 1 (Ti rich) and zone 3 (Ag rich) and a slightly higher resistivity values in zone 2. The piezoelectricity of the different samples are very similar and presented values from 19.6 6 pC N^{-1} to 27.6 pC N^{-1}.

Acknowledgments

The authors gratefully acknowledge the funding form the Portuguese national funds through the FCT- Fundação para a Ciência e a Tecnologia, (project SFRH/BD/71259/2010). Also thank support by FEDER through the COMPETE Program and by the Portuguese Foundation for Science and Technology (FCT) in the framework of the Strategic Project PEST-C/FIS/UI607/2011 and the project Matepro –Optimizing Materials and Processes", ref. NORTE-07-0124-FEDER-000037", co-funded by the "Programa Operacional Regional do Norte" (ON.2 – O Novo Norte), under the "Quadro de Referência Estratégico Nacional" (QREN), through the "Fundo Europeu de Desenvolvimento Regional" (FEDER).

References

[1] C. Oliveira, L. Gonçalves, B.G. Almeida, C.J. Tavares, S. Carvalho, F. Vaz, et al., XRD and FTIR analysis of Ti–Si–C–ON coatings for biomedical applications, Surf. Coatings Technol. 203 (2008) 490–494. doi:10.1016/j.surfcoat.2008.06.121.

[2] R. Branemark, P.-I. Branemark, B. Rydevik, R.R. Myers, Osseointegration in skeletal reconstruction and rehabilitation, J. Rehabil. Res. Dev. 38 (2001) 1–8.

[3] S.P. Mohanty, E. Kougianos, Biosensors: a tutorial review, Potentials, IEEE. 25 (2006) 35–40.

[4] V. Correia, V. Sencadas, M.S. Martins, C. Ribeiro, P. Alpuim, J.G. Rocha, et al., Piezoresistive sensors for force mapping of hip-prostheses, Sensors Actuators A Phys. 195 (2013) 133–138.

[5] P. Alpuim, V. Correia, E.S. Marins, J.G. Rocha, I.G. Trindade, S. Lanceros-Mendez, Piezoresistive silicon thin film sensor array for biomedical applications, Thin Solid Films. 519 (2011) 4574–4577. doi:10.1016/j.tsf.2011.01.300.

[6] V. Correia, C. Caparros, C. Casellas, L. Francesch, J.G. Rocha, S. Lanceros-Mendez, Development of inkjet printed strain sensors, Smart Mater. Struct. 22 (2013) 105028. doi:10.1088/0964-1726/22/10/105028.

[7] J. Nunes-Pereira, V. Sencadas, V. Correia, J.G. Rocha, S. Lanceros-Méndez, Energy harvesting performance of piezoelectric electrospun polymer fibers and polymer/ceramic composites, Sensors Actuators A Phys. 196 (2013) 55–62. doi:10.1016/j.sna.2013.03.023.

[8] J.G. Rocha, L.M. Gonçalves, P.F. Rocha, M.P. Silva, S. Lanceros-Mendez, Energy Harvesting From Piezoelectric Materials Fully Integrated in Footwear, Ind. Electron. IEEE Trans. 57 (2010) 813–819. doi:10.1109/TIE.2009.2028360.

[9] P. Martins, A.C. Lopes, S. Lanceros-Mendez, Electroactive phases of poly(vinylidene fluoride): Determination, processing and applications, Prog. Polym. Sci. 39 (2014) 683–706. doi:10.1016/j.progpolymsci.2013.07.006.

[10] V.K. Tiwari, P.K. Kulriya, D.K. Avasthi, P. Maiti, Radiation-resistant behavior of poly(vinylidene fluoride)/layered silicate nanocomposites., ACS Appl. Mater. Interfaces. 1 (2009) 311–8. doi:10.1021/am800040q.

[11] C.J. Tavares, S.M. Marques, L. Rebouta, S. Lanceros-Mendez, V. Sencadas, C.M. Costa, et al., PVD-Grown photocatalytic TiO2 thin films on PVDF substrates for sensors and

actuators applications, Thin Solid Films. 517 (2008) 1161–1166. doi:10.1016/j.tsf.2008.06.024.

[12] S.M. Marques, C.J. Tavares, S. Lanceros-Mendez, Z. Denchev, X-ray Scattering Experiments on Sputtered Titanium Dioxide Coatings onto PVDF Polymers for Self-Cleaning Applications, J. Appl. Polym. Sci. 119 (2011) 726–731. doi:10.1002/app.

[13] C.F.A. Alves, F. Oliveira, I. Carvalho, a. P. Piedade, S. Carvalho, Influence of albumin on the tribological behavior of Ag–Ti (C, N) thin films for orthopedic implants, Mater. Sci. Eng. C. 34 (2014) 22–28. doi:10.1016/j.msec.2013.09.031.

[14] C. Lopes, C. Gonçalves, P. Pedrosa, F. Macedo, E. Alves, N.P. Barradas, et al., TiAgx thin films for lower limb prosthesis pressure sensors: Effect of composition and structural changes on the electrical and thermal response of the films, Appl. Surf. Sci. 285 (2013) 10–18. doi:10.1016/j.apsusc.2013.07.021.

[15] N. Cerca, S. Martins, G.B. Pier, R. Oliveira, J. Azeredo, The relationship between inhibition of bacterial adhesion to a solid surface by sub-MICs of antibiotics and subsequent development of a biofilm, Res. Microbiol. 156 (2005) 650–655. doi:10.1016/j.resmic.2005.02.004.

[16] B. Jansen, K.G. Kristinsson, S. Jansen, G. Peters, G. Pulverer, In-vitro efficacy of a central venous catheter complexed with iodine to prevent bacterial colonization., J. Antimicrob. Chemother. 30 (1992) 135–139.

[17] H. Cao, X. Liu, F. Meng, P.K. Chu, Biological actions of silver nanoparticles embedded in titanium controlled by micro-galvanic effects, Biomaterials. 32 (2011) 693–705. doi:10.1016/j.biomaterials.2010.09.066.

[18] P.J. Kelly, H. Li, K. a. Whitehead, J. Verran, R.D. Arnell, I. Iordanova, A study of the antimicrobial and tribological properties of TiN/Ag nanocomposite coatings, Surf. Coatings Technol. 204 (2009) 1137–1140. doi:10.1016/j.surfcoat.2009.05.012.

[19] D.M. Eby, H.R. Luckarift, G.R. Johnson, Hybrid Antimicrobial Enzyme and Silver Nanoparticle Coatings for Medical Instruments, ACS Appl. Mater. Interfaces. 1 (2009) 1553–1560. doi:10.1021/am9002155.

[20] P. Pedrosa, C. Lopes, N. Martin, C. Fonseca, F. Vaz, Electrical characterization of Ag:TiN thin films produced by glancing angle deposition, Mater. Lett. 115 (2014) 136–139. doi:10.1016/j.matlet.2013.10.044.

[21] P. Pedrosa, E. Alves, N.P. Barradas, N. Martin, P. Fiedler, J. Haueisen, et al., Electrochemical behaviour of nanocomposite Agx:TiN thin films for dry biopotential electrodes, Electrochim. Acta. 125 (2014) 48–57. doi:10.1016/j.electacta.2014.01.082.

[22] P. Pedrosa, D. Machado, C. Lopes, E. Alves, N.P. Barradas, N. Martin, et al., Nanocomposite Ag:TiN thin films for dry biopotential electrodes, Appl. Surf. Sci. 285 (2013) 40–48. doi:10.1016/j.apsusc.2013.07.154.

[23] C. Gonçalves, C. Lopes, C. Fonseca, A. Guedes, F. Vaz, Structural and morphological evolution in TiAgx thin films as a function of in-vacuum thermal annealing, (n.d.).

[24] M. Ohring, The Materials Science of Thin Films, 2nd ed., Academic Press, San Diego, 2002.

[25] W.M. Posadowski, Sustained self sputtering dc magnetron materials using dc magnetron, Vacuum. 46 (1995) 1017–1020.

[26] J.C. Sánchez-López, M.D. Abad, I. Carvalho, R. Escobar Galindo, N. Benito, S. Ribeiro, et al., Influence of silver content on the tribomechanical behavior on Ag-TiCN bioactive coatings, Surf. Coat. Technol. 206 (2012) 2192–2198. doi:10.1016/j.surfcoat.2011.09.059.

[27] M. Li, C. Li, F. Wang, W. Zhang, Experimental study and thermodynamic assessment of the Ag–Ti system, Comput. Coupling Phase Thermochem. 29 (2005) 269–275. doi:10.1016/j.calphad.2005.09.002.

[28] J.L. Murray, K.J. Bhansali, The Ag-Ti (Silver-Titanium) System Ag-Ti, Bull. Alloy Phase Diagrams. 4 (1983) 178–183.

[29] D.A. Young, Phase diagrams of the elements, Lawrence L, University of California, 1975.

[30] J. Gomes, J. Serrado Nunes, V. Sencadas, S. Lanceros-Mendez, Influence of the β-phase content and degree of crystallinity on the piezo- and ferroelectric properties of poly(vinylidene fluoride), Smart Mater. Struct. 19 (2010) 065010 (7pp). doi:10.1088/0964-1726/19/6/065010.

[31] T. de los Arcos, P. Oelhafen, U. Aebi, a Hefti, M. Düggelin, D. Mathys, et al., Preparation and characterization of TiN–Ag nanocomposite films, Vacuum. 67 (2002) 463–470. doi:10.1016/S0042-207X(02)00232-4.

[32] R. Escobar Galindo, N.K. Manninen, C. Palacio, S. Carvalho, Advanced surface characterization of silver nanocluster segregation in Ag-TiCN bioactive coatings by RBS, GDOES, and ARXPS., Anal. Bioanal. Chem. 405 (2013) 6259–69. doi:10.1007/s00216-013-7058-z.

[33] V.S.K. Chakravadhanula, C. Kübel, T. Hrkac, V. Zaporojtchenko, T. Strunskus, F. Faupel, et al., Surface segregation in TiO2-based nanocomposite thin films., Nanotechnology. 23 (2012) 495701 (7 pp). doi:10.1088/0957-4484/23/49/495701.

[34] S.O. Kasap, Principles of Electronic Materials and Devices, McGraw-Hill Companies, 2002.

Figure Captions

Figure 1 – Variation of Ti and Ag contents (at.%) with the current density ratio (J_{Ag}/J_{Ti}).

Figure 2 - XRD patterns of $Ti_{1-x}Ag_x$ coatings deposited with different Ag/Ti atomic ratios (Cu Kα radiation). Magnifications of the XRD patterns are shown in Figure 2b.

Figure 3 – SEM micrographs on SE mode of different $Ti_{1-x}Ag_x$ thin films deposited on PVDF representative of the three different zones. The inceptions are micrographs in BSE mode for coatings Ag/Ti (0.11), Ag/Ti (0.69) and Ag/Ti (3.71).

Figure 4 - AFM images of coatings on silicon substrate with a scan range of 5 μm × 5 μm.

Figure 5 – Relationship between sheet resistivity (■), piezoelectric coefficients (d_{33}) (□) and the Ag content of the different thin films.

Tables

Table 1– Chemical composition, resistivity, roughness of $Ti_{1-x}Ag_x$ coatings and some experimental details.

Table 1

Coating	Zone	J_{Ti} (mA/cm^2)	J_{Ag} (mA/cm^2)	J_{Ag}/J_{Ti}	Deposition rate (nm/h)	Chemical Composition (at. %)		Ag/Ti	Resistivity (Ω/sq)	Roughness (nm)
						Ti	Ag			
Ti		5■	0	0	437.2	100	0	0	10.62±0.48	5.30
Ag/Ti (0.02)	Z1	4□	0.05■	0.0125	590	98	2	0.02	20.30±0.12	
Ag/Ti (0.11)		7.5■	0.05□	0.0067	891.8	89.8	10.2	0.11	13.87±0.29	3.55
Ag/Ti (0.21)	Z2	5■	0.05□	0.01	507.0	82.7	17.3	0.21	27.09±1.13	
Ag/Ti (0.69)		3.5■	0.15□	0.043	336.7	59.2	40.8	0.69	28.05±0.17	1.97
Ag/Ti (1.27)	Z3	3■	0.25□	0.083	405.2	44	56	1.27	10.24±0.06	
Ag/Ti (1.70)		4■	0.5□	0.125	752.0	37.1	62.9	1.70	6.91±0.33	
Ag/Ti (3.71)		2.5■	0.5□	0.2	629.6	21.2	78.8	3.71	4.21±0.11	3.42
Ag		0	2.5■	-	658.6	0	100	-	0.12±0.01	3.93

Figure 1

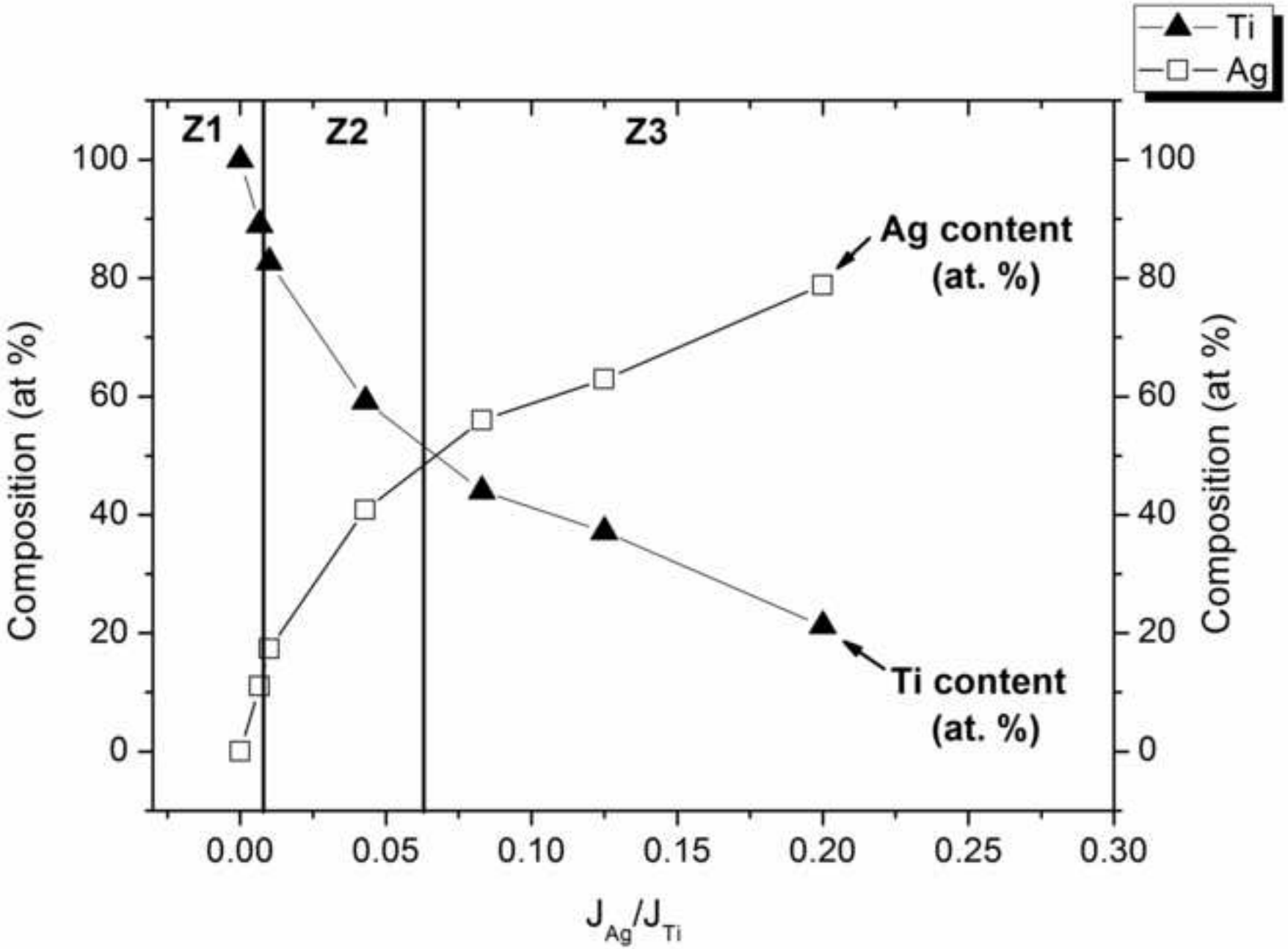
Ti
Ag
Z1
Z2
Z3
Ag content
(at. %)
Ti content
(at. %)
Composition (at %)
Composition (at %)
100
80
60
40
20
0
0.00
0.05
0.10
0.15
0.20
0.25
0.30
J_{Ag}/J_{Ti}

Figure 2a

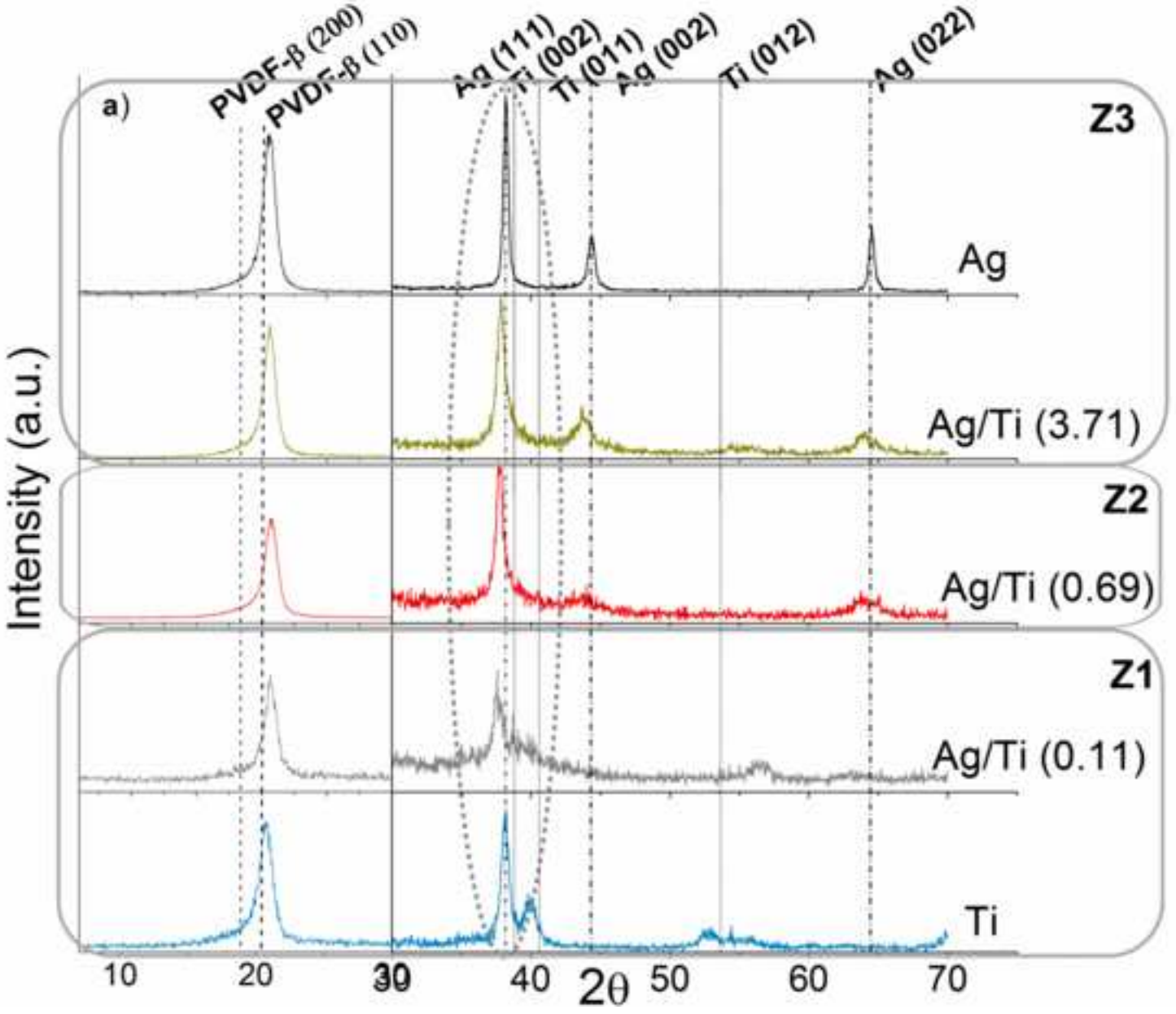
a)
PVDF-β (200)
PVDF-β (110)
Ag (111)
Ti (002)
Ti (011)
Ag (002)
Ti (012)
Ag (022)
Z3
Ag
Ag/Ti (3.71)
Z2
Ag/Ti (0.69)
Z1
Ag/Ti (0.11)
Ti
Intensity (a.u.)
10
20
30
40
2θ
50
60
70

Figure 2b

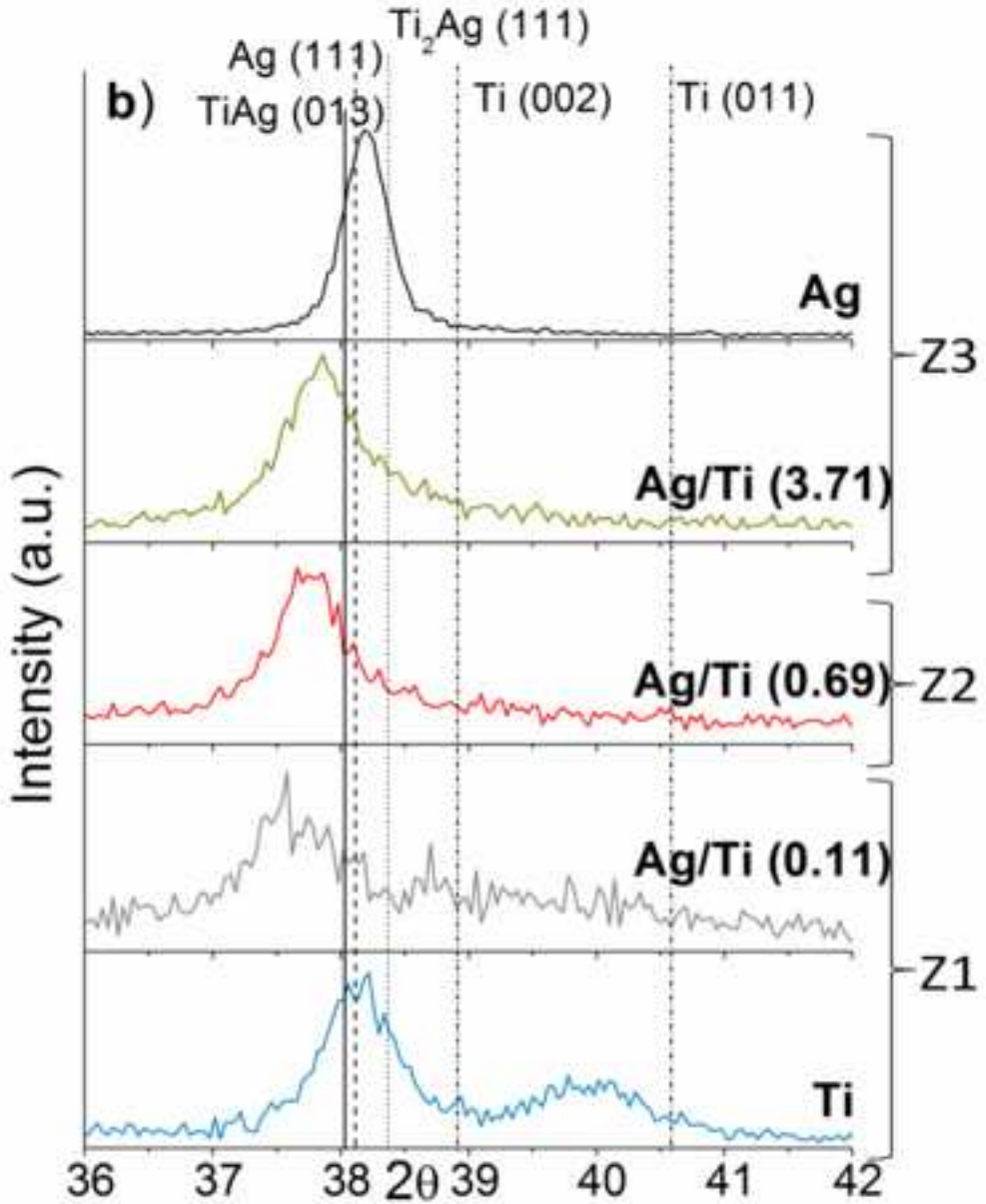
b)
Ag (111)
TiAg (013)
Ti2Ag (111)
Ti (002)
Ti (011)
Ag
Ag/Ti (3.71)
Ag/Ti (0.69)
Ag/Ti (0.11)
Ti
Z3
Z2
Z1
Intensity (a.u.)
36
37
38
2θ
39
40
41
42

Figure 3

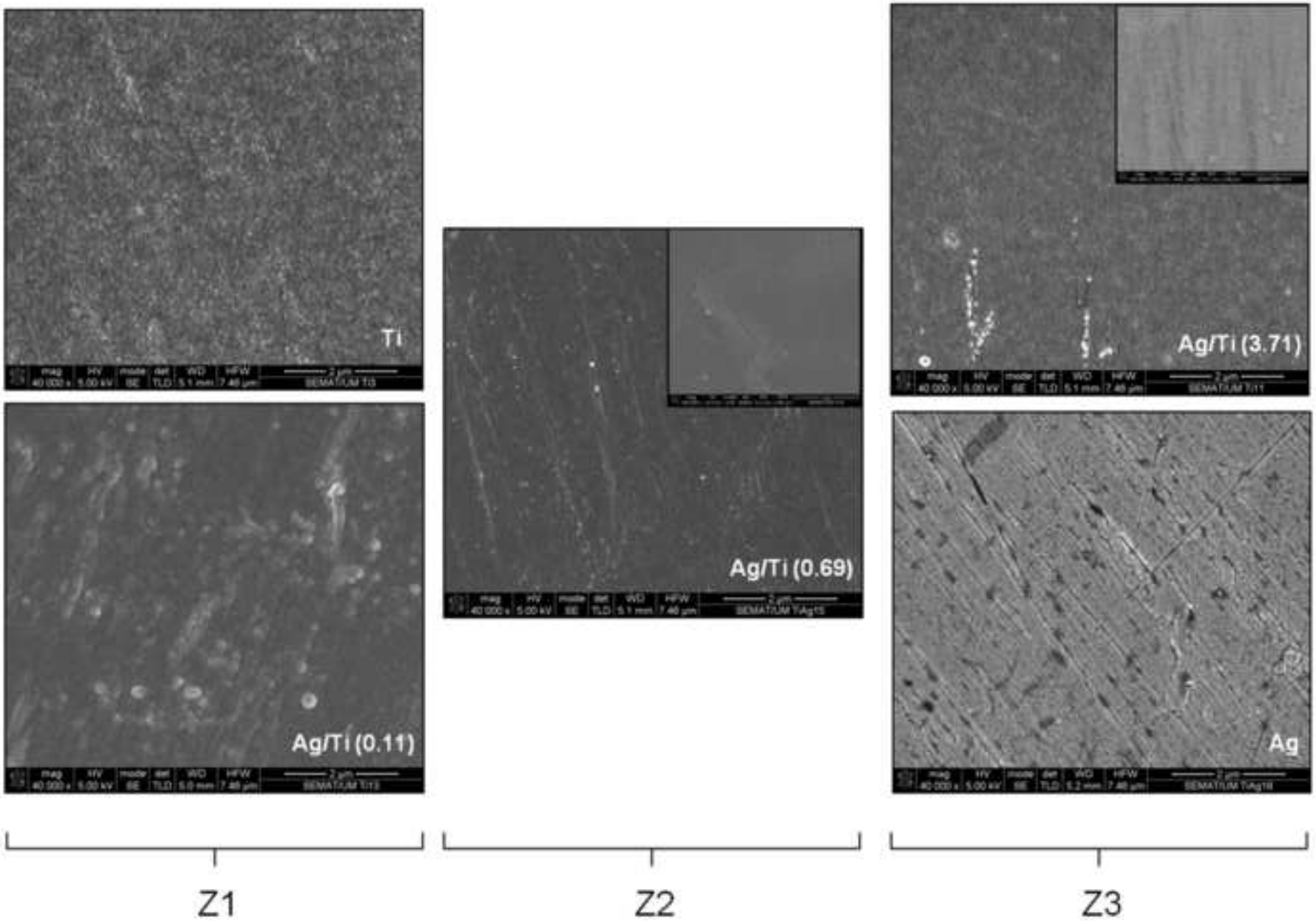

Figure 4

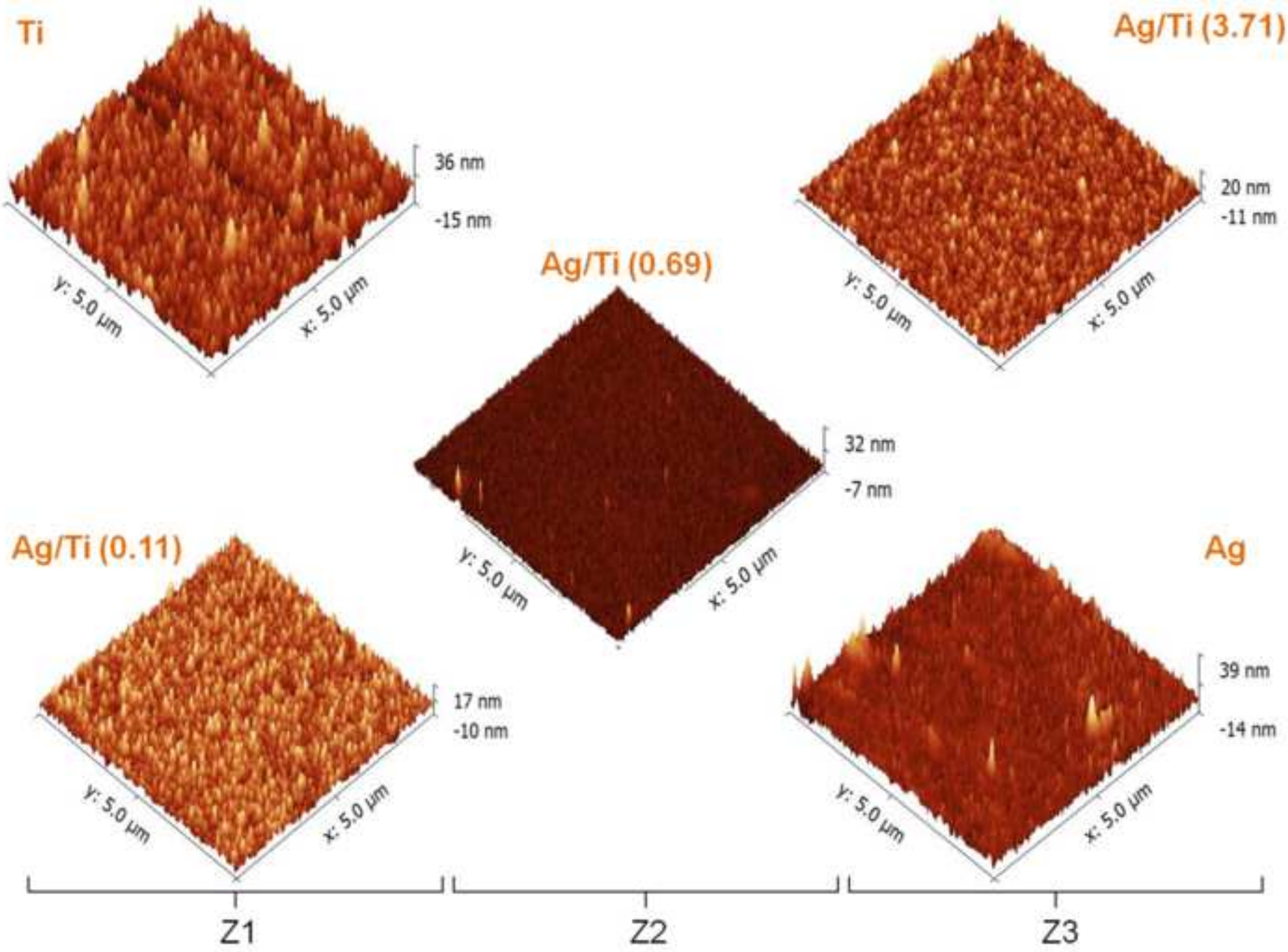
Ti
36 nm
-15 nm
y: 5.0 µm
x: 5.0 µm
Ag/Ti (3.71)
20 nm
-11 nm
y: 5.0 µm
x: 5.0 µm
Ag/Ti (0.69)
32 nm
-7 nm
y: 5.0 µm
x: 5.0 µm
Ag/Ti (0.11)
17 nm
-10 nm
y: 5.0 µm
x: 5.0 µm
Ag
39 nm
-14 nm
y: 5.0 µm
x: 5.0 µm
Z1
Z2
Z3

Figure 5

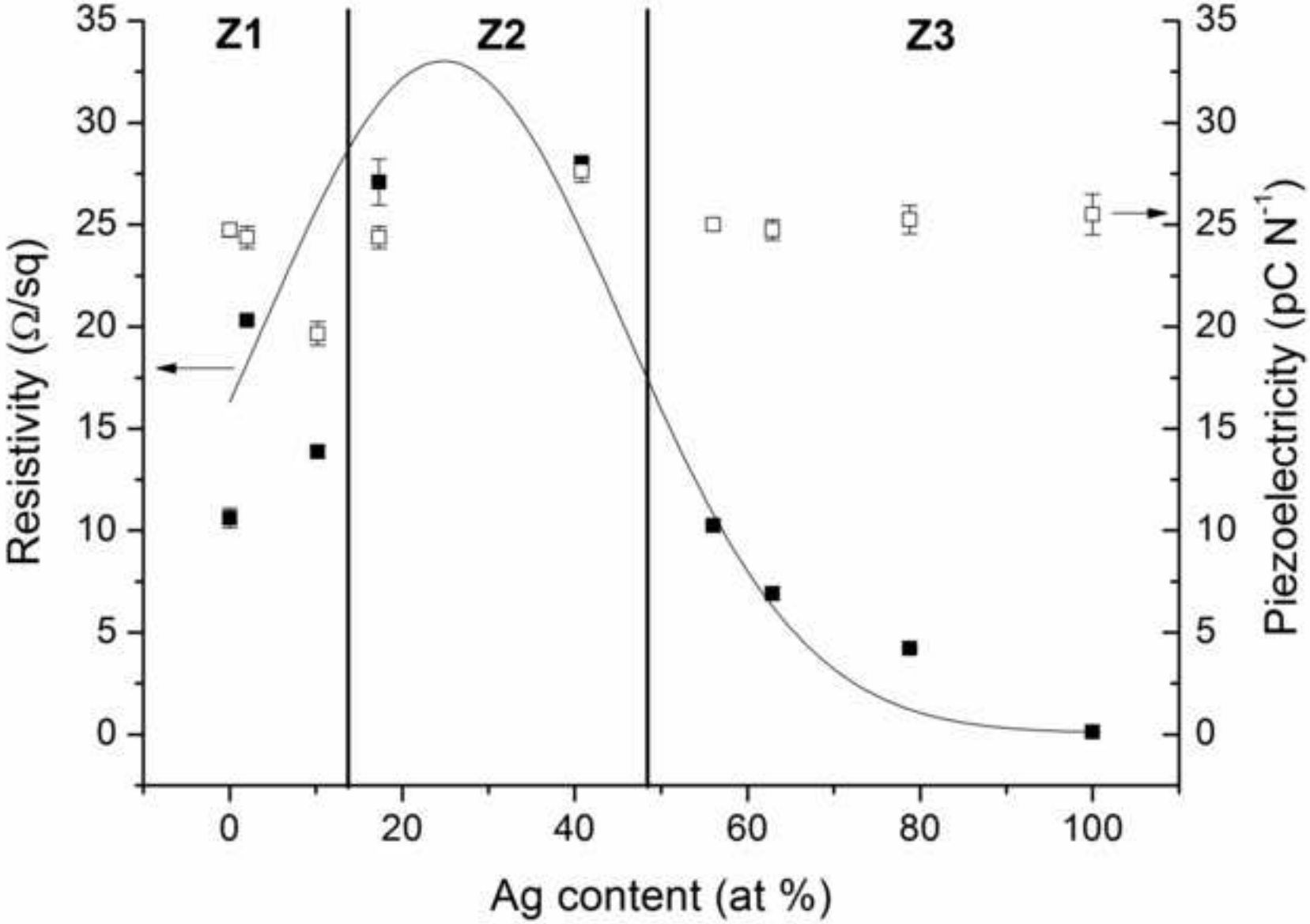
Z1
Z2
Z3
Resistivity (Ω/sq)
Piezoelectricity (pC N^{-1})
Ag content (at %)
0
5
10
15
20
25
30
35
0
20
40
60
80
100